Electrocardiograms and Heart Arrhythmia Detection

Arianna Badilla, Callie Cheung, Mohammed Karim, Anjelica Nojadera, Shan Vo

Department of Bioengineering, University of California, San Diego

***Abstract* - The mechanics of the heart are measured by a series of electrical activities that correspond to the different phases of the heart. This electrical activity - typically denoted as different types of waves - can be measured by an electrocardiogram to determine heart behavior. Abnormalities of the heart can be detected by high peaks as well as abnormal QRS complex times. The following circuit aims to appropriately measure the QRS complexes of the heart and filter out abnormal heart behavior. Through the use of Falstad, a circuit simulator, the circuit was tested using both normal and abnormal QRS complexes to demonstrate appropriate circuit behavior. Individual portions of the circuit were tested and satisfied gain specifications as measured by expected output voltage (12.01V) and were capable of filtering out noise based on desired cutoff frequencies.**

***Keywords*— Heart Arrhythmias, QRS Complexes, Electrocardiogram, Instrumentation Amplifier, Signal Conditioning**

I. INTRODUCTION

The QRS complex represents the electrical impulses as it spreads through the ventricles and it indicates ventricular depolarization. The normal heart beats in a rhythmic fashion with a P wave, QRS wave, and T wave. The Q wave indicates the first negative deflection from the baseline. The R wave indicates the first positive deflection following the Q wave. Finally, the S wave shows the first negative deflection below baseline following the R wave [1]. In normal QRS complexes, the rhythm is initiated from a site above the ventricles and lasts around 0.08 to 0.10 seconds. For an abnormal QRS complex with a duration greater than 0.12 seconds, it appears wider and bizarre with a slurred/notched spike. Abnormal QRS complexes are produced by abnormal depolarization of the ventricles and possible factors include ventricular hypertrophy, intraventricular conduction disturbance, or ventricular pacing by the cardiac pacemaker [1]. Our focus on tall QRS complexes are commonly caused by hypertrophy of one or both ventricles [2]. Low-voltages in QRS complexes can often be seen in obese and hyperthyroid patients.

Our goal was to determine and investigate heart abnormalities using a bandpass filter. More specifically, we are identifying heart abnormalities with a high R complex [3]. Heart abnormalities usually occur due to electrical impulses not working properly, which means that the heart is either beating too fast or beating too slow or irregularly. The most common cause for high R complexes indicate posterior myocardial infarction or PMI which is when the posterior coronary circulation becomes disturbed [3].

Although posterior myocardial infarction alone is not very common, occurring around 3-11% of the population, PMI often accompanies ST-elevation myocardial infarction, which is a serious heart attack where one of the major arteries are blocked. PMI accompanying ST-elevation myocardial infarction affects 15-20% of the population [4].

We decided to design a system utilizing an electrocardiogram (ECG) to record the electrical activity of the heart where the QRS complex and the ECG signals will correspond to events in the heart. ECGs are a very common tool in clinical practice for measuring the rhythms of the heart beat and with these signals and variations in the QRS complex it can help diagnose heart abnormalities, in which for our specific design. We will be using the ECG to identify high R complexes, which can lead us to a common cause of PMI. Difficulties in using ECGs include external noise as it can attribute to the signals recorded, which is why we wanted to implement a band pass filter.

II. METHODS

a. DESIGN OVERVIEW

i. Functional Requirements

We wanted to design a three-frontal lead ECG bioamplifier system that would produce six amplified leads I, II, III, aVR, aVL, and AVF to filter the expected frequency range for a human heartbeat, focusing purely on the QRS complex. The system takes as input the three skin electrodes RA, LA, and RL, located on the right shoulder, left shoulder, and right hip respectively, and outputs the ECG amplified voltage of any one of the six frontal ECG leads. Furthermore, the design includes a single instrumental amplifier (IA) and a filtering stage

from a low-pass filter to a high-pass filter. As a design constraint, we also set the current to be no more than $10\ \mu A$ running through the patient.

ii. Block Diagram

The following design is composed of a measurand, transducer, signal conditioning, and output. The measurand, which is any physical quantity that the system measures [5], is the electrical activity of the heart. More specifically, this project's emphasis is on the QRS complexes and their magnitude. With respect to the transducer, the goal is to convert the measured electrical activity into a voltage that functions within the circuit. The signal conditioning phase involves both an instrumentation amplifier to largely increase the gain of the signal, as well as a set of filters meant to remove any noise picked up by the system while maintaining the gain setup in the amplification phase. Finally, the circuit would output a voltage that can be read and understood by a technician to indicate high complexes. As such, this display would be a graphical representation of the complexes (as is shown in the results section).

b. CIRCUIT

i. Circuit Overview

The circuit acts as an electrocardiogram that acquires signals corresponding to an individual's cardiac rhythm. The signals first pass through an instrumentation amplifier followed by a bandpass filter constructed using a low pass filter cascaded to a high pass filter. Each stage of the circuit will be described further below.

ii. The Instrumentation Amplifier

The instrumentation amplifier shown in Figure 1 functions to process the signals received from the skin electrodes and amplify them for further signal conditioning. For the analysis of the instrumentation amplifier, the following assumptions are made:

1. Assume that all operational amplifiers are ideal and provide infinite gain.

2. Assume that all tolerance values in the instrumentation amplifier fall within $\pm 1\%$.

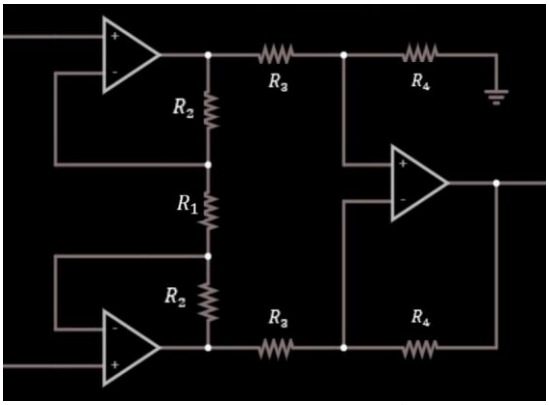

Figure 1: Instrumentation amplifier.

Instrumentation Amplifier Component Values	
Circuit Component	Component Values
R_1	500Ω
R_2	$300K\Omega$
R_3	$1K\Omega$
R_4	$100K\Omega$

Table 1: Resistor values associated with the instrumentation amplifier displayed in Figure 1.

Using the resistor values in *Table 1* above and Equations 1-3 from the Appendix, the instrumentation amplifier produces a differential gain $A_d \approx 120{,}100$, a common mode gain $A_c \approx 4$, and a common mode rejection ratio $CMRR(dB) \approx 89.55\,dB$. The large differential gain indicates the ability of the amplifier to boost weak signals, while the CMRR represents the amplifier's ability to reject common-mode interference that may otherwise alter the output signal.

iii. The Bandpass Filter Stage

Following the instrumentation amplifier, a bandpass filtering stage was constructed by implementing a 2nd-order, Sallen-Key low-pass filter followed by a 2nd-order, Sallen-Key high-pass filter. These are shown below in *Figures 2* and *3* respectively.

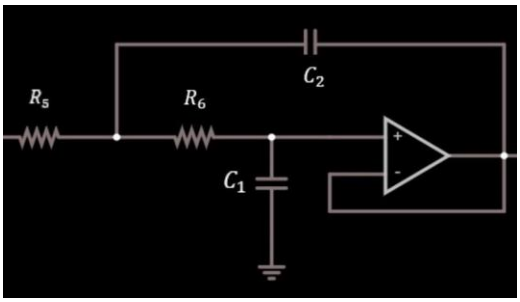

Figure 2: 2nd-order low-pass filter immediately following the instrumentation amplifier.

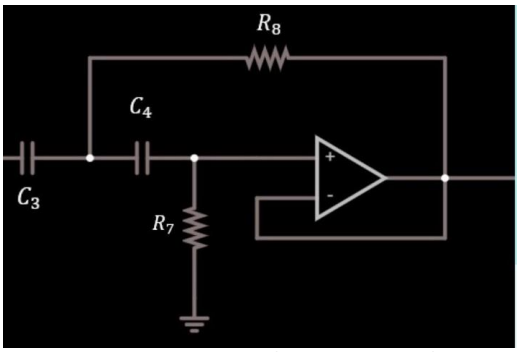

Figure 3: 2nd-order high-pass filter immediately following the low-pass filter from Figure ?

The cutoff frequencies of the filters were determined through recommendations from literature and research articles. While a typical human heartbeat ranges from 40-120 beats per minute (bpm), or 0.67-2Hz, adhering to this range for ECG waveform generation causes major distortions to the final signal [6,7]. Because of this, the American Heart Association (AHA) suggests that the appropriate frequency range for a standard ECG is 0.05-100Hz [6,7,8]. These values were used as the high-pass and low-pass cutoff frequencies $f_{c,HP}$ and $f_{c,LP}$. From these frequency values, the circuit component values for both of the filters were determined using Equation (6) of the Appendix and are provided in *Table 2* below.

Bandpass Filter Component Values	
Circuit Component	Component Values
R_5, R_6	$16K\Omega$
R_7, R_8	$33K\Omega$
C_1, C_2	$0.1\mu F$
C_3, C_4	$100\mu F$

Table 2: Circuit component values associated with the instrumentation amplifier displayed in Figure 1

III. RESULTS

Due to the scope of the project, we were unable to pass a single, continuous waveform through the completed circuit that emulates the appropriate amplitudes and frequencies associated with an adult heartbeat. Rather, each circuit component was evaluated separately depending on their intended function. This will be discussed in detail below.

iv. The Instrumentation Amplifier

As stated previously, the instrumentation amplifier functions to provide a large gain for the initial signals acquired from the body. To verify the gain calculations, a waveform generator was utilized to administer AC sine waveforms of identical 40 Hz frequencies to mimic the measurands acquired from the right and left arm respectively. The maximum voltage values were determined by identifying the typical voltage range of an ECG reading, which falls within 0.1mV-5mV [1]. The positive voltage input from the left arm was assigned a maximum voltage value of 1.1mV, while the negative voltage output from the right arm was assigned a maximum value of 1mV. Figure 4 below shows the initial waveform in green and the final amplified waveform in red, bringing the maximum voltage value from 1.1mV to 11.855V. From our differential gain $A_d \approx 120{,}100$, a voltage input difference of 0.1mV should yield an expected output voltage $v_o \approx 12.01V$. Here, we see that the circuit is able to satisfy the estimated voltage value, indicating that the instrumentation amplifier provides sufficient gain to the heartbeat signals. Furthermore, these results verify the ability of the amplifier to amplify signals of interest.

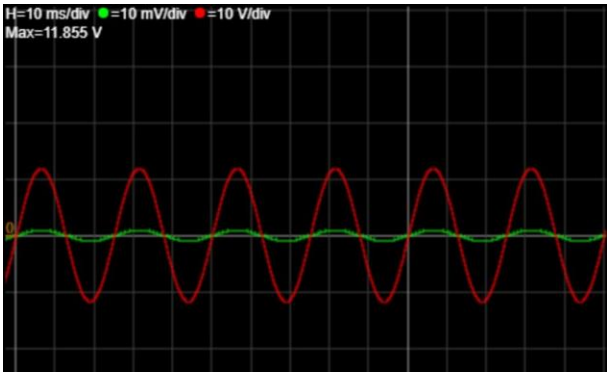

Figure 4: 2nd-order high-pass filter immediately following the low-pass filter from Figure ?

v. The Bandpass Filter

To analyze the bandpass filter, the transfer functions of the low pass filter $H(j\omega)_{LP}$ and the high pass filter $H(j\omega)_{HP}$ were derived, as shown below and in Equations (4) and (5) of the Appendix:

$$H(j\omega)_{LP} = \frac{1}{1 + j\omega C_1(R_5 + R_6) + R_5R_6C_1C_2(j\omega)^2}$$

$$H(j\omega)_{HP} = \frac{C_3C_4R_7R_8(j\omega)^2}{1 + j\omega R_8(C_3 + C_4) + C_3C_4R_7R_8(j\omega)^2}$$

Using these equations and the values from *Table 1*, the Bode plots in *Figures 5-6* were visualized in MATLAB to observe the behavior of both filters. The Bode plot for each filter is shown in blue, while the intended cutoff frequencies are indicated in orange. Here, each curve corresponds with the cutoff frequencies $f_{c,HP} \approx 0.05Hz$ and $f_{c,LP}f_{c,LP} \approx 100Hz$ required of a standard ECG. The result of these plots indicate that our design is equipt to isolate the proper frequencies values needed for the signals of interest.

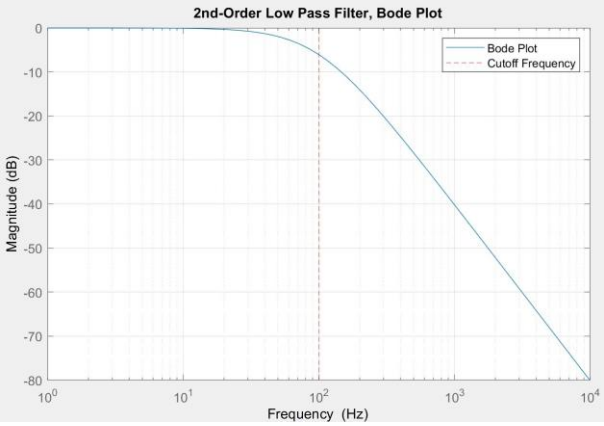

Figure 5: 2nd-order low-pass filter Bode plot with a cutoff frequency $f_{c,LP} = 99.47\ Hz \approx 100Hz$

Figure 6: 2nd-order high-pass filter Bode plot with a cutoff frequency $f_{c,HP} = 0.04829\ Hz \approx 0.05Hz$

IV. ADVANTAGES AND LIMITATIONS

From our design we had placed the ECG skin electrodes directly on the surface of the epidermis, one of the few advantages that were utilized would be attaching additional silver-chloride electrodes and contact gel onto the patient's skin. This will allow the signal strength of the electrodes to increase by gently reducing skin resistance and easier signal detection from the electrical activity within the heart. The implementation of a high-pass filter permits unwanted noise to be filtered out, while maintaining clear readings on the other electrical signals and movement present. Through applying a low-pass filter within the circuit design excess high frequencies are then removed from the record. Low frequencies are also removed from the use of a high-pass filter.

An instance of limitations within this particular design would be the utilization of active filters, which have tendencies to be inaccurate when calculating the instantaneous spikes or ripples in the bandpass. If the correct components are not selected from the active filters the data collection would be recording unwanted ripples or activity in the passband or stopband, along with unwanted phase shifts in certain frequencies or QRS complex peaks. In the instance where the component value is not accurately collected the result would be the filtering of unwanted frequencies and inaccurate measurement of electrical activity in the heart. This overall would cause the detection of abnormalities of the heart activity to be inconsistent with the current irregular patterns or nonuniform electrical impulses. Within this design there is also the use of only one single lead which limits the full scope of the electrical activity and restricts the amount of peaks that can be detected from the patient.

Additionally, a major limitation to verifying the functionality of our design was not being able to pass a continuous waveform through the circuit with the appropriate frequency and magnitude values associated with an adult human heartbeat. This would allow us to evaluate the aspects of our circuit design altogether and produce realistic output signals. Additionally, the suggested AHA frequency range for adults was used to determine our cutoff frequencies. Therefore, the design is only suited for adults. Pediatric cases require a high pass cutoff as high as 250Hz and 150Hz for adolescents [7]. Modifications would need to be made if the system is used by younger individuals.

.

V. CONCLUSION

A few future improvements that could be made would be comparing the QRS complexes along with the P and T waves, rather than only observing the QRS complexes. This broadens the overall pattern of the

heart's electrical activity. Our design is also only suited for adults as we utilize a higher voltage than a design for a child would be. This factor of the design does not take into account the differing heart patterns that younger children may have in comparison to older patients. Another consideration that could be made would be the implementation of a more precise method of filtering the frequency, in order to prevent any incorrect data collection of inaccurate ripples that do not represent the QRS complex as well to avoid any false denoting of phase shifts or frequencies. However, as per our specifications, the circuit system functioned appropriately and satisfied gain specifications as well as satisfying cutoff frequencies consistent with those found in literature.

VI. ACKNOWLEDGEMENTS

We thank Professor Gert Cauwenbergh for his suggestions and feedback. We thank TAs Preston Fowler, Qin Li, and Anuja Girish Walke for their guidance and support. Their efforts, examples, and continuous encouragement has helped us improve our design, stimulate our creativity, and refine the overall structure of our research on ECGs and heart arrhythmia detection.

VII. REFERENCES

[1] Normal ecg. (n.d.). Retrieved March 18, 2021, from https://elentra.healthsci.queensu.ca/assets/modules/ECG/normal_ecg.html#:~:text=T%20wave%20deflection%20should%20be,in%20leads%20V5%20and%20V6

[2] Ungar1, L. (2019, June 07). ECG primer for the Cath: What does a TALL R wave in V1 Mean? The four categories approach. Retrieved March 18, 2021, from https://www.cathlabdigest.com/content/ecg-primer-cath-what-does-tall-r-wave-v1-mean-four-categories-approach

[3] Wolpert, C., Veltmann, C., Schimpf, R., Antzelevitch, C., Gussak, I., & Borggrefe, M. (2008, September). Is a narrow and tall QRS complex an ECG marker for SUDDEN DEATH? Retrieved March 18, 2021, from https://www.ncbi.nlm.nih.gov/pmc/articles/PMC2570045/

[4] What is a STEMI? (2016, April 29). Retrieved March 18, 2021, from https://www.ecgmedicaltraining.com/what-is-a-stemi/

[5] Webster JG, *Medical Instrumentation: Application and Design*, 4th ed., John Wiley & Sons: New York, 2010.

[6] F. Buendía-Fuentes, M. A. Arnau-Vives, A. Arnau-Vives, et al. "High-Bandpass Filters in Electrocardiography: Source of Error in the Interpretation of the ST Segment," Vol. 12, Jun. 21, 2012. https://www.hindawi.com/journals/isrn/2012/706217/

[7] P. Kligfield, L. S. Gettes, J. J. Bailey, et al. "Recommendations for the Standardization and Interpretation of the Electrocardiogram," vol. 15, no. 10, Feb. 23, 2007. https://www.ahajournals.org/doi/10.1161/circulationaha.106.180200

[8] J. J. Bailey, A. S. Berson, A. Garson et al., "Recommendations for standardization and specifications in automated electrocardiography: bandwidth and digital signal processing. A report for health professionals by an ad hoc Writing Group of the Committee on electrocardiography and Cardiac Electrophysiology of the Council on Clinical Cardiology, American Heart Association," Circulation, vol. 81, no. 2, pp. 730–739, 1990.

VIII. APPENDIX [5]

Differential Gain [5]

The differential gain A_d of the instrumentation amplifier can be solved in the following way:

$$\text{Differential Gain: } A_d \approx -(1 + 2\frac{R_2}{R_1})(\frac{R_4}{R_3}) \quad (1)$$

where R_1, R_2, R_3,and R_4 are each resistors with values outlined in Table 1.

Common Mode Gain [5]

The common mode gain A_c of the instrumentation amplifier is:

$$\text{Common Mode Gain: } A_c \approx 0 \pm 0.04(\frac{R_4}{R_3}) \quad (2)$$

where $R_3$and R_4 are each resistors with values outlined in Table 1.

Common Mode Rejection Ratio [5]

The common mode rejection ratio expressed in decibels $CMRR(dB)$is calculated using the equation:

$$CMRR(dB) \approx 20log(\frac{|A_d|}{A_c}) \quad (3)$$

where A_d is the differential gain from Eqn. 1 and A_c is the common mode gain from Eqn. 2.

Transfer Functions for 2nd-Order Filters

Given the Sallen-Key topology of both the low-pass and high pass filters, the transfer functions in the frequency domain for each filter are as follows:

$$H(j\omega)_{LP} = \frac{1}{1+j\omega C_1(R_5+R_6)+R_5R_6C_1C_2(j\omega)^2} \quad (4)$$

$$H(j\omega)_{HP} = \frac{C_3C_4R_7R_8(j\omega)^2}{1+j\omega R_8(C_3+C_4)+C_3C_4R_7R_8(j\omega)^2} \quad (5)$$

where $R_5, R_6, R_7, R_8, C_1, C_2, C_3$and C_4 are each resistors with values outlined in Table 2.

Cutoff Frequency Equation

From Eqns. (4) & (5), the cutoff frequency for each filter are expressed by the following equation:

$$f_c = \frac{1}{2\pi\sqrt{R_AR_BC_AC_B}} \quad (6)$$

where R_A, R_B, C_A, and C_B are the corresponding resistor and capacitor coefficients of the highest order term in the denominator of the transfer function.